strain
An International Journal for Experimental Mechanics

Acoustic Emissions at High and Low Frequencies During Compression Tests in Brittle Materials

A. Schiavi*, G. Niccolini*, P. Tarizzo*, A. Carpinteri†, G. Lacidogna† and A. Manuello†

*National Research Institute of Metrology, INRIM, Strada Delle Cacce 91, 10135 Torino, Italy

†Politecnico di Torino, Department of Structural Engineering and Geotechnics, Corso Duca Degli Abruzzi 24, 10129 Torino, Italy

ABSTRACT: The damage process in a concrete specimen subjected to uniaxial compression test is investigated by detection of the propagating elastic waves because of micro- and macrocrack growth. Besides the high-frequency acoustic emissions (AEs), the presence of low-frequency elastic emissions (ELEs), from 1 to 10 kHz, is detected just before the specimen failure. A spectral analysis of the ELEs is performed by measuring with a calibrated transducer the local acceleration of the specimen surface. Quantitative information about the macrocrack effects in terms of released energy is thus obtained. Furthermore, the evolution of damage is followed through the analysis of the amplitude distribution of AE and ELE signals, distributed according to the Gutenberg–Richter (GR) statistics.

KEY WORDS: *acoustic emissions, b-value analysis, elastic emissions, fracture precursors, low-frequency*

Introduction

The mechanical behaviour and the damage evolution of heterogeneous materials under compressive loading conditions are of great interest. Acoustic emission (AE) because of crack growth in brittle materials is usually observed in the high frequency (HF) range, typically from 10^2 to 10^3 kHz, since the beginning of the damage process. The AE detection is used for damage localisation and damage level assessment in quasi-brittle materials such as concrete and rocks [1–5]. The increasing rate in the AE activity is observed as the specimen approaches impending failure, and it is correlated with the progressive degradation of mechanical properties of material (decrease of the Young modulus) [6–13].

It is established by numerous investigations that the AE activity varies during damage process. The AEs released in various stages of this process are distinguished by its own energy and furthermore are concentrated in various sections of the frequency range; at the start of the damage process (microcrack initiation), AE is emitted at high frequencies, and later (microcrack coalescence into cracks of large length), the AE frequencies drop off to few kHz or less [13, 14].

In this perspective, the attention is focused also on the characterisation of low-frequency (LF) elastic emissions (ELEs), specifically in the range of 1–10 kHz, detected in a concrete specimen under compression.

The goal is analysing two well-separated frequency ranges of emitted signals to investigate the different stages of damage process (microcrack initiation and macrocrack growth), which precede the failure of quasi-brittle materials.

Elastic Wave Propagation in High- and Low-Frequency Ranges

Crack growth in a rigid stressed-strained specimen causes redistribution of the internal stresses in the form of transient elastic waves. Therefore, each crack event acts as an impulsive force that causes elastic vibrations of the specimen. During nucleation and growth of microcracks, high-frequency acoustic emissions (AE) are observable. As soon as microcracks coalesce to form cracks of large length, the frequencies drop off and ELE clearly appear in addition to AE [13, 14].

In the case of AE, the longitudinal and/or shear wave propagation is because of the oscillations of material particles around their equilibrium positions during microcrack growth (Figure 1A). While the growth of large cracks, forming new internal surfaces, is accom-

doi: 10.1111/j.1475-1305.2010.00745.x

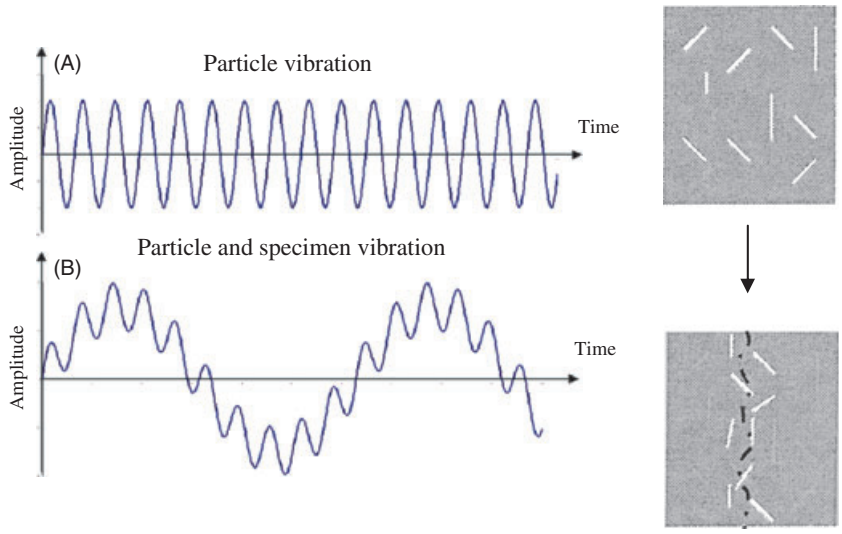

Figure 1: (A) Schematic representation of AE because of particle vibration around their equilibrium position; (B) schematic representation of ELE because of relevant oscillations of the entire specimen and typical related patterns at the initial and final stage of failure process

panied by high-amplitude and long-wavelength elastic vibrations (ELE), which are able to deform the bulk of the solid and break its continuity (Figure 1B).

Testing Equipment and Measurement Methods

A $0.1 \times 0.1 \times 0.1$ m^3 concrete specimen (ρ = 2200 kg m^{-3}) with 10-mm maximum-aggregate-size and average ultimate strength of 47.07 MPa is analysed under uniaxial compression conditions. The test is performed in displacement control at constant piston velocity of 0.5 μm s^{-1}, using a servo-hydraulic press (Figure 2A) with a maximum capacity of 500 kN, equipped with control electronics. The specimen adheres to the press platens without any coupling material (specimen–platen contact with friction).

Two kinds of PZT transducers, working in two different and well-separated frequency ranges, are attached to the surface of the specimen to detect variation in frequency signal components in the spectrum during damage process (Figure 2B).

The first kind is a PZT strainmeter working in the range of 50–500 kHz, designed for detection of AE events, which are characterised by the output response of the transducer, expressed in volts. Although a calibration diagram fulfilling metrological requirements of the adopted PZT transducers has yet to be determined, the electrical signal can be assumed to be proportional to the acceleration at the specimen surface over the considered frequency range and thus be used to quantify signal amplitude.

The second one is a 'delta shear' accelerometer, working in the range of 1–10 kHz for detection of ELE events. In this case, the events are characterised by the output response of the calibrated transducer (charge sensitivity 9.20 pC m^{-1} s^{-2}), expressed in

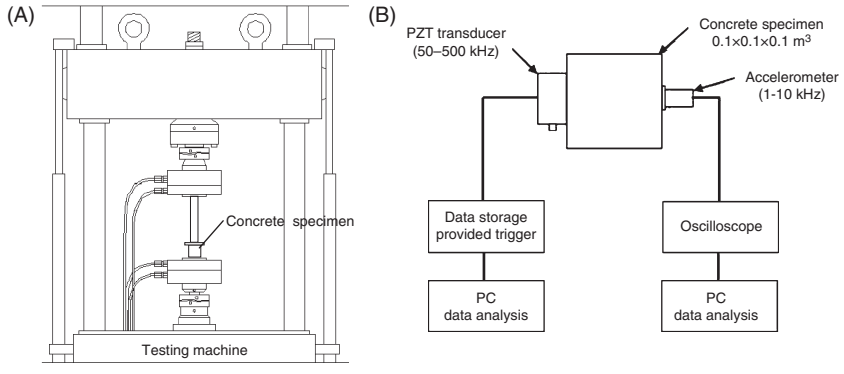

Figure 2: (A) Testing machine constituted by a standard servo-hydraulic press. (B) PZT transducers and 'delta shear' accelerometers applied to the external surfaces of the concrete tested specimen

doi: 10.1111/j.1475-1305.2010.00745.x

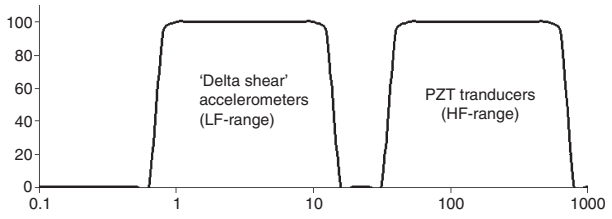

Figure 3: Frequency bands of sensitivity for the transducers used in the experimental test

mm s^{-2}. The accelerometer transducer behaves as a damped mass on a spring, and this oscillation is used to give a calibrated reading to the surface acceleration.

The maximum sensitivity for the PZT strainmeter and the accelerometer is shown in Figure 3, where in particular it can be noted the linear frequency response of 'delta shear' accelerometer range from 1 to 10 kHz.

To filter out environmental background noise, we set appropriate detection thresholds for both acquisition systems, respectively, fixed at 200 μV for AE signals and 40 dB (referred to 1 μm s^{-2}) for ELE signals. In this way, we verify that no spurious signals are detected before the beginning of the test. Furthermore, we proceed to the identification and quantification of the mechanical noise of the press in the low-frequency range during the test. In this frequency range, the mechanical noise has an average value of about 62 ± 2 dB, with three well-pronounced peak levels between 50 and 53 dB at 2.5, 5.3 and 5.8 kHz (Figure 4).

Experimental Results and AE Data Analysis

The mechanical response of the specimen during the compression test is linear until failure, which thus occurs abruptly without any apparent accumulation of damage (Figure 5A); however, an increasing AE and ELE activity in amplitude and rate (see also Figure 5B,C) reveals the existence of a damage process developing during the specimen compression.

At the beginning of damage process, signals are emitted only at high frequencies, indicating microcrack initiation. Later on, the increase in the AE rate is accompanied by the appearance of ELE activity at lower frequencies, suggesting both an increase in the density of microcracks and their coalescence into large cracks. Finally, during the last seconds of the specimen life, an abrupt increase in the ELE rate is accompanied by a sudden drop in the AE rate, revealing that the final stage of damage process is dominated by the propagation of large cracks leading to the specimen failure (Figure 5A).

It is noteworthy that the acquisition of AE signals is performed storing a set of signal parameters (i.e. the arrival time and the peak amplitude), whereas that of ELE signals is performed storing the complete waveforms. Thus, ELE signals are subjected to spectral analysis and plotted in time–frequency–amplitude coordinates.

Figure 6A represents a time window at the start of the damage process, characterised by sporadic signals with energy content concentrated in a narrow frequency band; the ELE spectrum at time t_1 = 2457 s inside this window has a peak level of 62 dB and a global level of 77 dB (Figure 7A).

Figure 6B represents a time window just before the specimen failure, characterised by numerous signals with much higher energy content spread over the entire frequency interval. The spectrum of ELE activity at time t_2 = 3424 s inside this window has a peak level of 100 dB and a global level of 115.0 dB (Figure 7B).

It can be observed that the background noise is negligible, being <1% of ELE signals, whose acceleration spectral levels range between 80 and 120 dB.

The time histories of peak frequencies and amplitudes are split into two parts (see the dashed line in Figure 8) corresponding to two different stages of damage process. In the first part, the peak frequencies range between 4.8 and 5.8 kHz (Figure 8A), and the peak amplitudes between 60 and 75 dB (Figure 8B). In the second part, a sudden drop in the frequency domain and an abrupt increase in the amplitude levels are associated with much higher ELE rate (compare Figures 5A and 8). Therefore, the frequency drop in ELE signals seems to be correlated with the coalescence of microcracks forming the through-

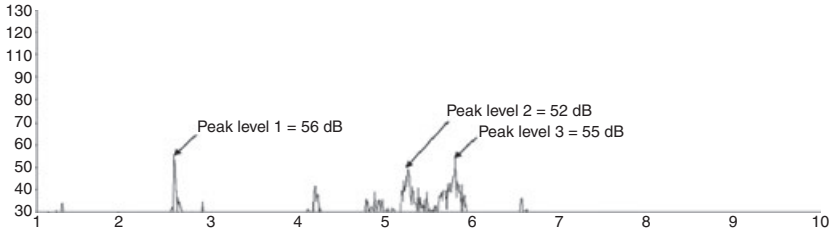

Figure 4: Global level of the background noise vibration

doi: 10.1111/j.1475-1305.2010.00745.x

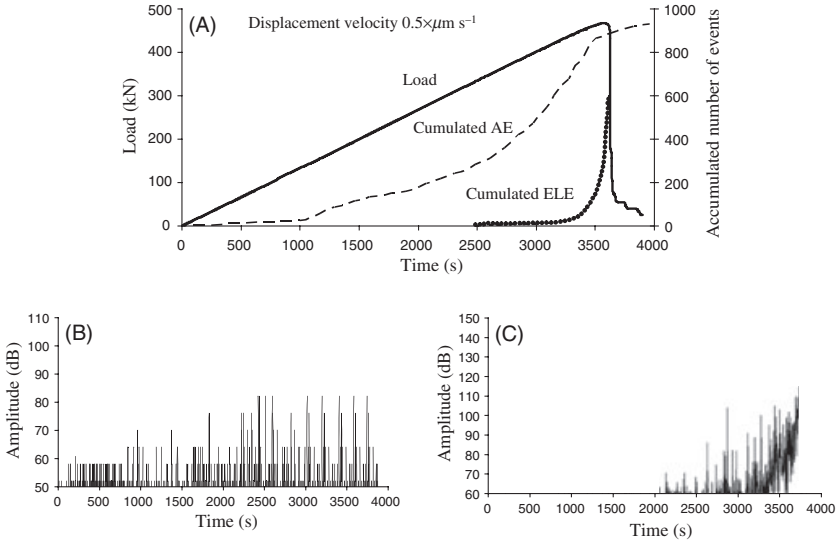

Figure 5: (A) Load history until failure of the concrete specimen, accumulated number of AE and ELE events versus time; (B) time series of AE and (C) ELE events

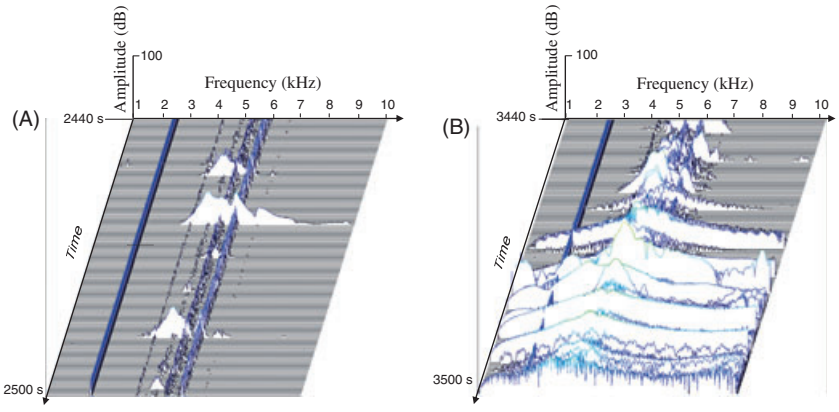

Figure 6: Spectral analysis of ELE activity in two time windows (A) at the start of damage process and (B) just before the failure

going fracture surfaces. This evidence suggests that ELE frequency analysis is a valuable tool for damage level assessment.

AE and ELE Frequency–Magnitude Statistics

The most important phenomenological law describing the amplitude scaling of emission events is the GR law [15–21]:

$$\mathrm{Log}N(\geq m) = a - bm \qquad (1)$$

where $N(\geq m)$ is the number of events with magnitude $M \geq m$ occurring in the specimen volume during a given time interval, and b (or 'b-value') indicates the damage level reached in the specimen. The magnitude of AE events is defined in dB through the relation $\log(V_{max}/1\ \mu\mathrm{V})$; the magnitude of ELE events is defined in dB through the relation $20\ \log(a_{max}/1\ \mu\mathrm{m\ s^{-2}})$.

The b-value, being correlated with the degree of damage localisation, is recognised as a useful tool for damage level assessment. In general terms, the damage process moves from diffused microcracking to localised macrocracks as the material approaches impending failure, and the b-value decreases from values in the range (1.5–2.5) at the initial stages to values approximately 1, and less, during propagation of the through-going fracture [16–21].

Subdividing the loading process into different stages, the trend of the related b-values versus time is plotted in Figure 9 for both AE and ELE. All detected events are partitioned into groups of 100 events, calculating for each group the b-value, as previous studies show that using groups formed by a number of events between 70 and 130 does not substantially modify the results [16]. Remarkably, both AE and ELE b-values show a decreasing trend towards a final

doi: 10.1111/j.1475-1305.2010.00745.x

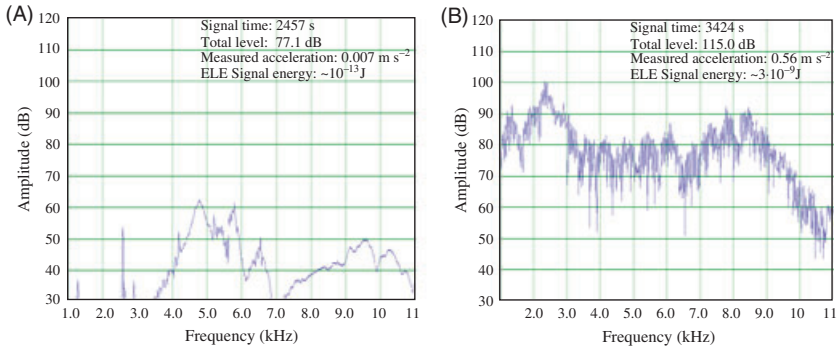

Figure 7: Spectral analysis of ELE at 2757 and 3424 s

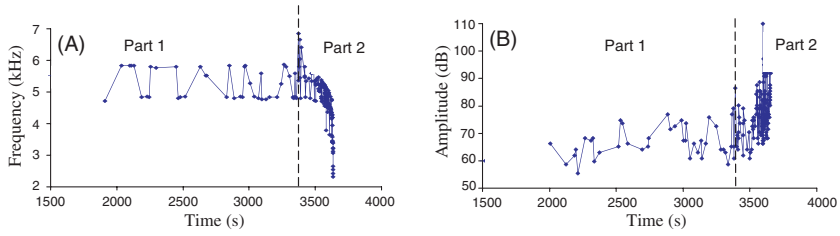

Figure 8: (A) time history of peak frequencies and (B) peak amplitudes of ELE signals

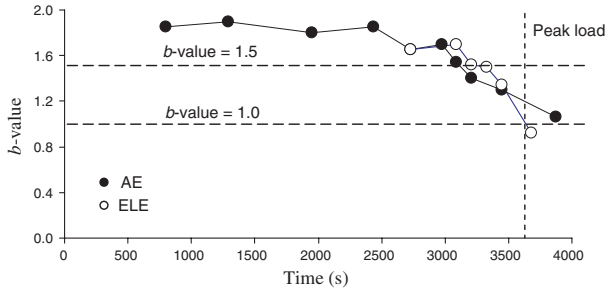

Figure 9: Trends of the *b*-value versus time computed for AE and ELE signals

value close to 1 just before the specimen failure, in agreement with previous citation studies.

Conclusions

In this work, the damage process occurring in a concrete specimen under compression is studied by means of elastic energy release because of crack growth. In particular, elastic emissions (ELE) in the frequency range 1–10 kHz are detected and analysed. In the last stages of the test, the abrupt increase in the ELE count rate likely describes the transition from diffused microcracking to localised macrocracks which characterises failure process in quasi-brittle materials. Other signatures of damage evolution are observed, such as the frequency drop in ELE signals and the decrease in GR *b*-value.

ACKNOWLEDGEMENTS

The financial support provided by the European Union (EU) Leonardo da Vinci Programme, ILTOF Project is gratefully acknowledged. Special thanks are due to Mr Vincenzo Di Vasto of the Politecnico di Torino. The authors are also grateful to Dr Eng. Andrea Pavoni Belli and to Dr Andrea Agosto of the National Research Institute of Metrology – INRIM.

REFERENCES

1. Shah, S. P. and Li, Z. (1994) Localisation of microcracking in concrete under uniaxial tension. *ACI Mater. J.* **91**, 372–381.
2. Ohtsu, M. (1996) The history and development of acoustic emission in concrete engineering. *Mag. Concrete Res.* **48**, 321–330.
3. Scholz, C. H. (1968) Microfracturing and the inelastic deformation of rock in compression. *J. Geophys. Res.* **73**, 1417–1432.
4. Ohnaka, M. and Mogi, K. (1982) Frequency characteristics of acoustic emissions in rocks under uniaxial compression and its relation to the fracturing process to failure. *J. Geophys. Res.* **87**, 3873–3884.
5. Landis, E. N. and Shah, S. P. (1995) Frequency-dependent stress wave attenuation in cement-based materials. *J. Engrg. Mech.* **121**, 737–743.
6. Anzani, A., Binda, L., Carpinteri, A., Lacidogna, G. and Manuello, A. (2008) Evaluation of the repair on multiple leaf stone masonry by acoustic emission. *Mater. Struct. (RILEM)* **41**, 1169–1189.
7. Carpinteri, A. and Lacidogna, G. (2006) Damage monitoring of an historical masonry building by the Acoustic Emission technique. *Mater. Struct.* **39**, 161–167.

doi: 10.1111/j.1475-1305.2010.00745.x

8. Carpinteri, A. and Lacidogna, G. (2006) Structural monitoring and integrity assessment of medieval towers. *J. Struct. Eng. (ASCE)* **132**, 1681–1690.
9. Carpinteri, A. and Lacidogna, G. (2007) Damage evaluation of three masonry towers by Acoustic Emission. *Eng. Struct.* **29**, 1569–1579.
10. Carpinteri, A., Invernizzi, S., Lacidogna, G., Manuello, A. and Binda, L. (2008) Numerical simulation and monitoring of the Cathedral of Siracusa in Sicily. *6th International Conference on Structural Analysis of Historical Construction*, Bath 2–4 July 2008.
11. Carpinteri, A., Invernizzi, S., Lacidogna, G., Manuello, A. and Binda, L. (2009) Stability of the vertical bearing structures of the Syracuse Cathedral: Experimental and numerical evaluation. *Mater. Struct.* **42**, 877–888.
12. Turcotte, D. L., Newman, W. I. and Shcherbakov, R. (2003) Micro and macroscopic models of rock fracture. *Geophys. J. Int.* **152**, 718–728.
13. Krajcinovic, D.. (1996) *Damage Mechanics*, Elsevier, Amsterdam.
14. Kukalov, G. I. and Yakovitskaya, G. E. (1993) Acoustic emission and stages of the crack-formation process in rock. *Mining Institute, Siberian Branch, Russian Academy of Sciences, Novosibirsk*, **2**, 111–114.
15. Richter, C. F. (1958) *Elementary Seismology*. W.H. Freeman, San Francisco.
16. Colombo, S., Main, I. G. and Forde, M. C. (2003) Assessing Damage of Reinforced Concrete Beam Using '*b*-value' Analysis of Acoustic Emission Signals. *J. Mater. Civil Eng. (ASCE)* **15**, 280–286.
17. Sammonds, P. R., Meredith, P. G. and Main, I. G. (1992) Role of pore fluid in the generation of seismic precursors to shear fracture. *Nature* **359**, 22–230.
18. Rao, M. V. M. S. and Lakschmi, P. K. J. (2005) Analysis of b-value and improved b-value of acoustic emissions accompanying rock fracture. *Curr. Sci. (Bangalore)* **89**, 1577–1582.
19. Carpinteri, A., Lacidogna, G., Niccolini, G. and Puzzi, S. (2008) Critical defect size distributions in concrete structures detected by the Acoustic Emission technique. *Meccanica* **43**, 349–363.
20. Carpinteri, A., Lacidogna, G. and Manuello, A.. The *b*-value analysis for the stability investigation of the ancient Athena Temple in Syracuse. *Strain* doi: 10.1111/j.1475-1305.2008.00602.x.
21. Shiotani, T., Yuyama, S., Li, Z. W. and Othsu, M. (2000) *Quantitative* Evaluation of Fracture Process in Concrete by the Use of Improved *b*-value. *5th Int. Symposium Non-Destructive Testing in Civil Engineering*. Elsevier Science, Amsterdam, 293–302.